Glassy behavior in an exactly solved spin system with a ferromagnetic transition

Robert L. Jack,[1] Juan P. Garrahan,[2] and David Sherrington[1]
[1]*Rudolf Peierls Centre for Theoretical Physics, University of Oxford, 1 Keble Road, Oxford, OX1 3NP, United Kingdom*
[2]*School of Physics and Astronomy, University of Nottingham, Nottingham, NG7 2RD, United Kingdom*
(Received 1 October 2004; published 11 March 2005)

We show that applying simple dynamical rules to Baxter's eight-vertex model leads to a system which resembles a glass-forming liquid. There are analogies with liquid, supercooled liquid, glassy, and crystalline states. The disordered phases exhibit strong dynamical heterogeneity at low temperatures, which may be described in terms of an emergent mobility field. Their dynamics are well described by a simple model with trivial thermodynamics, but an emergent kinetic constraint. We show that the (second order) thermodynamic transition to the ordered phase may be interpreted in terms of confinement of the excitations in the mobility field. We also describe the aging of disordered states toward the ordered phase, in terms of simple rate equations.

DOI: 10.1103/PhysRevE.71.036112 PACS number(s): 64.60.−i, 64.70.Pf, 05.50.+q

INTRODUCTION

Despite many years of study of glass-forming liquids, the most suitable paradigm in which to discuss the "glass transition" and its associated dynamical phenomena remains controversial. In recent years, there has been progress [1–3], driven by the idea that the dynamical properties of glass formers may be characterized by a zero temperature dynamical fixed point [2]. This is in contrast to the predictions of other theories which involve a finite temperature singularity in the dynamics [4,5] or the thermodynamics of the relevant system [6–8].

However, there remains an important qualitative difference between physical glass formers and the models, such as the Fredrickson-Andersen (FA) [9] or East [10] models (see Ref. [11] for a review) studied in Refs. [1–3]: the crystal phase is completely absent from these models. As a result, they are relevant if the glass-forming liquid is in a long-lived (but metastable) supercooled phase. Further, interplay between the thermodynamic singularity associated with the transition to the crystal and the dynamical fixed point associated with the glass is certainly possible, but the FA and East models cannot capture these phenomena since their thermodynamics are trivial. There has been recent work [12,13] (see also Ref. [14]) investigating these issues with regard to glassy systems, although without reference to a glassy fixed point at zero temperature.

The extent to which the FA and East models can be viewed as pictures of real glasses is therefore contingent on two main assumptions. First, the behavior of the supercooled state should not be affected by the proximity of the freezing transition, since the FA and East models regard glassy slowing down as a purely dynamical effect, not requiring a thermodynamic transition. Second, the "mobility field" represented by the spins in these models should emerge naturally from atomistic degrees of freedom of the glass former.

One class of models in which this latter effect is demonstrated are the two-dimensional plaquette models [15–17], in which an effective dynamical constraint emerges naturally from a simple spin model. There are free excitations in the spin field which are naturally interpreted as a mobility field. At temperatures lower than the glassy onset temperature T_o [3,18], the dynamics are strongly heterogeneous, and slow down rapidly with decreasing temperature.

In this paper, we address the other issue mentioned above: how are dynamics of metastable supercooled states affected by the presence of the freezing transition? We study dynamics in the eight-vertex model, whose thermodynamics were solved by Baxter [19]. The model may be treated as a generalization of the square plaquette model [15,17]; the effect of this generalization is to introduce a (second order) phase transition to an ordered state at a finite temperature T_c. We identify this with a freezing transition, and investigate the dynamics around this transition. The transition temperature T_c may be varied with respect to the glassy onset temperature T_o. This fact, together with the exactly solved thermodynamics, gives an extra degree of control to our simulations.

We will show that we may prepare long-lived "supercooled" states below T_c, whose dynamics are controlled by the effective dynamical constraint of the plaquette model, and are not affected by the freezing transition for times shorter than the lifetime of the supercooled state.

To be more precise, the dynamics of the system within the supercooled state resemble those of strong glasses, and arise from diffusing pointlike excitations in a mobility field [1–3]. Considering supercooled states at different temperatures, we find that they obey dynamical scaling consistent with a zero-temperature fixed point. The presence of the ferromagnetic transition means that these states have a finite lifetime, but it does not affect the dynamics on time scales shorter than this lifetime. This is consistent with the assumptions made when modeling glass formers using models without an ordering transition [1–3].

The form of the paper is as follows. In Sec. I, we describe the model, identify relevant energy scales and their hierarchy, and discuss the relation between the spins of our model and the atomistic degrees of freedom of a physical glass former. We discuss the nature of the ordered and disordered phases of the model system in Sec. II: we then use this information to interpret simulations of the dynamics of the model in Sec. III. Finally, we summarize our results and discuss their significance for models of the glass transition.

I. THE MODEL

The zero-field eight-vertex model solved by Baxter [19] may be expressed either in terms of its original vertices, or as an Ising model with Hamiltonian

$$H = \sum_{ij} [-D\sigma_{ij}\sigma_{i+1,j}\sigma_{i,j+1}\sigma_{i+1,j+1} - J(\sigma_{ij}\sigma_{i+1,j+1} + \sigma_{i+1,j}\sigma_{i,j+1})] \tag{1}$$

where the $\{\sigma_{ij}\}$ are Ising spins on a square lattice. We note that the Ising coupling is between *next nearest* neighbors on the square lattice: at $D=0$ there are two independent sublattices, with Ising coupling J within each sublattice. There is a transition at $J=(T/2)\sinh^{-1}(1)$ to a fourfold degenerate ordered state (there are two ferromagnetic and two antiferromagnetic ground states, related by flipping all the spins on either sublattice). As D is increased from zero, the lattices become coupled, and the transition moves to a higher temperature: the critical temperature T_c satisfies

$$\sinh(2J/T_c) = \exp(-2D/T_c). \tag{2}$$

The transition to an ordered state occurs for all finite J: we also note that if $D>J$ then the transition temperature will be much larger than J.

Thus far we have considered only static (thermodynamic) properties of the eight-vertex model. In order to study the time evolution of this model, we must specify dynamical rules. We use simple spin flips with rates given by Glauber dynamics. We refer to the combination of the Hamiltonian and the dynamical rules as the spin-flip eight-vertex (SEV) model.

If we set $J=0$ in the SEV model, we arrive at the (two-dimensional) plaquette model [15,20,21]. In this limit there is no ordering at any finite temperature: all two-point static correlations vanish. This may be most easily demonstrated by noting that if $J=0$ then the Hamiltonian is invariant under flipping all of the spins in any row or column of the square lattice. The dynamics of this model are dominated by a zero-temperature dynamical fixed point for temperatures T that are small compared to D. Since we are studying slow dynamics we work throughout at $T<D$.

We have now identified two temperature scales in the problem: the onset of glassy dynamics occurs at $T=T_o\sim D$ and the critical point in the system is at $T=T_c$. If $T_c>T_o$ then we expect the slow dynamics to be observable only in the ordered phase: the more interesting case is $T_o>T_c$, in which case the dynamics are slow near the transition, and we may investigate the effect of the effective kinetic constraint as we cool the system through T_c. We therefore work at $T_c<D$: from Eq. (2), this means that $J<T_c$. As a result we have the hierarchy $J<(T,T_c)<D$ which is obeyed throughout this paper.

Relation of this work to physical glass formers

Before investigating the SEV model more closely, we establish the relationship between this model and physical glass formers: it is not obvious at first sight precisely how a model of Ising spins should be related to an atomistic system. The spin variables represent the microscopic degrees of freedom of the glass former. This is distinct from the more heuristic approach taken in the FA and East models in which the spins represent a coarse-grained "mobility field." The SEV model is more similar to the plaquette model [17] in that the effective kinetic constraint responsible for the critical slowing down at zero temperature is not inserted explicitly, but arises from the combination of the Hamiltonian and simple spin-flip dynamics. In Sec. III we will comment briefly on how the dynamics may be interpreted within a "mobility field" picture like that of the FA model.

In the previous section we identified the two temperature scales in the model as the glassy onset temperature $T_o\sim D$ and the transition temperature $T_c<T_o$. These separate the behavior of the system into three regimes. We argue that the high temperature phase of the SEV model with $T>(T_o,T_c)$ resembles a liquidlike state of the atomistic system, since it lacks any two-point correlations between the spins.

The second regime is $T_c<T<T_o$: there are still no static correlations between the spins but there are strong *dynamical* correlations. This state resembles a viscous liquid whose relaxation time is large compared to microscopic time scales. We emphasize that the crossover between this regime and the high temperature behavior is smooth: there is no sharp transition at T_o. In the viscous liquid, the atomistic degrees of freedom are "jammed" over large regions of the system: relaxation in these regions is frustrated by large energy barriers. Dynamical heterogeneity then arises naturally, due to the presence of mobile regions where the energy barriers are smaller than average. There are very many paramagnetic states in the spin system, even at low temperatures (compared to D): these resemble the many possible jammed states of the glass former.

Having argued that the paramagnetic phase of our model is liquidlike, and shows glassy behavior at low temperatures, it is natural to interpret the transition in the model as a freezing transition. We identify the ferromagnetic phase with the crystalline states of the glass former. As the temperature is lowered through T_c the entropy falls rapidly as the very many paramagnetic (jammed) states are now thermodynamically unstable with respect to the ferromagnet. The effect of the dynamical fixed point on the transition between paramagnet and ferromagnet is the main subject of the following sections. In particular we show that "supercooling" of the paramagnetic state is possible as long as $T_c \ll D$.

II. STATIC PROPERTIES OF THE SEV MODEL

We now discuss the microscopic structure of the ferromagnetic and paramagnetic states in the model of Eq. (1). This will allow us to identify the relevant correlation functions for our study of the dynamics of the system. We describe the paramagnetic state in terms of small deviations from the behavior of the model with $J=0$, and the ferromagnetic state in terms of excitations in an ordered background. This will lead us to interpret the transition in terms of free defects above T_c that become confined at the transition, forming composite excitations. We will also show that these descriptions are valid even rather close to the transition, de-

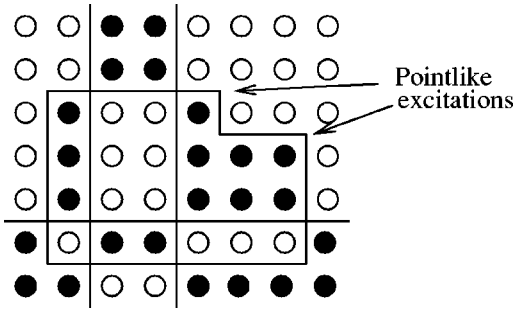

FIG. 1. Sketch showing the relation between spin states, excited plaquettes, and domain walls. Up (down) spins are represented by filled (empty) circles. Domain walls form closed loops with excited plaquettes (energy cost $2D$) at each isolated corner (there is no energy cost associated with wall crossings). A domain wall costs energy $2J$ per unit length when running through a ferromagnetically ordered region. Interactions between domain walls reduce this tension in disordered states.

spite being based on expansions around the fully ordered or fully disordered states. In other words, the critical region is very narrow.

We begin by recalling some results for the $J=0$ limit of the model [20,21]. At $J=0$, we write $p_i = \sigma_{ij}\sigma_{i,j+1}\sigma_{i+1,j}\sigma_{i+1,j+1}$, and the Hamiltonian reduces to

$$H_{J=0} = -D\sum_i p_i, \tag{3}$$

where the p_i are Ising-like degrees of freedom, defined on the plaquettes of the square lattice. In the thermodynamic limit, these plaquettes are independent degrees of freedom, which define the state of the spin system, up to transformations that flip all the spins in any row or column (leaving $H_{J=0}$ invariant). We observe that this results in a ground state entropy proportional to the linear size of the system, L (there are $N = L^2$ spins in the system).

In finite systems, the presence of boundary conditions may impose constraints on the plaquettes. For example, imposing periodic boundaries on the spins means that the number of excited plaquettes in all rows and columns must be even (we believe that this fact led to the strong finite size effects seen in Ref. [21]).

As discussed in Ref. [21], the low temperature states of the model with $J=0$ are best interpreted in terms of closed loops with excited plaquettes at each vertex (see Fig. 1). If we move across the lattice, any spin flip is accompanied by our crossing the perimeter of a loop. If $J=0$ then each plaquette is independent: the vertices of the loops are a free lattice gas with density $(1+e^{2D/T})^{-1}$. The free energy per site is simply

$$f_{J=0} = -T\ln[2\cosh(D/T)]. \tag{4}$$

At finite J, we make use of Baxter's solution of the eight-vertex model [19]. In the Appendix, we show that the free energy per site for $T \gg T_c$ is given approximately by

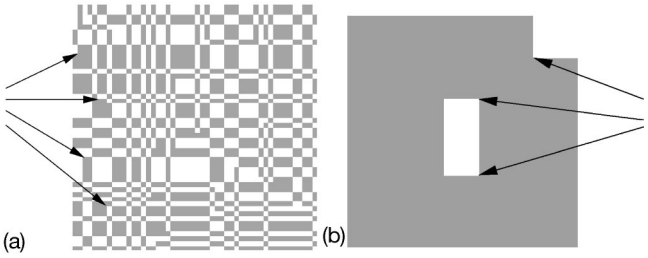

FIG. 2. Typical states of the spin system above (left) and below (right) T_c. Some of the excited plaquettes are identified by arrows. They are "free" above T_c, but "confined" on corners of rectangular excitations in the ferromagnetic phase.

$$f^{(0)}_{\mathrm{PM}} = -T\ln[e^{D/T}\cosh(2J/T) + e^{-D/T}]. \tag{5}$$

Since we work exclusively at $J<T$, Eq. (5) is rather close to the $J=0$ expression (4).

We focus on two correlation functions, the density of excited plaquettes n_p and the density of broken Ising bonds n_b. Their definitions are

$$n_p = \frac{1}{2}(1 - \langle \sigma_{ij}\sigma_{i,j+1}\sigma_{i+1,j}\sigma_{i+1,j+1}\rangle), \tag{6}$$

$$n_b = \frac{1}{4}(2 - \langle \sigma_{ij}\sigma_{i+1,j+1} + \sigma_{i+1,j}\sigma_{i,j+1}\rangle). \tag{7}$$

In the representation of Fig. 1, the concentration of vertices is given by n_p. The parameter n_b is related to the total perimeter of the closed loops of that figure, and measures the spatial ordering of the vertices. The free plaquettes observed at $J=0$ have $n_b=(1/2)$. As n_b is reduced, the reduction in the loop perimeter starts to constrain the positions of the vertices, and spatial correlations appear.

The internal energy per site is given by

$$\langle H/N\rangle = 2Dn_p + 4Jn_b - (D+2J) \tag{8}$$

so we have $n_p=(1+\partial f/\partial D)/2$ and $n_b=(2+\partial f/\partial J)/4$. Using Eq. (5), the paramagnetic state has

$$n_p \simeq [1 + e^{2D/T}\cosh(2J/T)]^{-1}, \tag{9}$$

$$n_b \simeq (1/2) - \frac{\sinh(2J/T)}{\cosh(2J/T) + e^{-2D/T}}. \tag{10}$$

We see that introducing J leads to small negative corrections to the $J=0$ values of n_p and n_b. However, for $T<D$, the concentration of excited plaquettes is still approximately $c = e^{-2D/T}$ and these plaquettes are only weakly interacting since $n_b \simeq (1/2)$. A typical configuration is shown in Fig. 2: there are no two-point correlations between the spins, but the loop vertices are dilute since $T \ll D$.

We now consider the system at temperatures lower than T_c. As shown in the Appendix, a good approximation to the free energy per site in the ferromagnetic phase is

$$f_{\mathrm{FM}}^{(0)} = -D - 2J - \frac{Te^{-8D/T}}{16\sinh^2(2J/T)} \tag{11}$$

which is valid for $J<T<T_c<D$. In this regime

$$n_p = \frac{e^{-8D/T}}{4\sinh^2(2J/T)}, \tag{12}$$

$$n_b = \frac{e^{-8D/T}}{16\sinh^2(2J/T)\tanh(2J/T)}. \tag{13}$$

For excitations in a ferromagnetic background, n_b is directly related to the perimeter of the closed loops shown in Fig. 1. Equations (12) and (13) are therefore consistent with rectangular excitation loops with an excited plaquette at each corner (total energy cost $8D$). The expectation of the loop perimeter is approximately $(T/2J)$. This is much smaller than the typical spacing between loops, given by $(8J/T)e^{4D/T}$. This situation is sketched in Fig. 2.

The density of loops is given by the number of ways of forming such a loop, multiplied by a Boltzmann factor $e^{-8D/T}$. We therefore identify the entropy per loop as $S_{\mathrm{loop}} \sim -2\ln[4\sinh(2J/T)]$. The apparent divergence of the perimeter (and therefore the entropy) at small J represents the breakdown of the ordered state which happens at T_c. The transition to the paramagnetic state occurs when the energy cost for adding two vertices to the loop ($4D$) is balanced by the entropy gain associated with adding an extra rectangular segment to the loop. This entropy gain is approximately S_{loop}. We may therefore obtain an estimate of the transition temperature by setting $4D/T_c = S_{\mathrm{loop}}$. The result is

$$4\sinh(2J/T_c) \simeq \exp(-2D/T_c), \tag{14}$$

which differs from the exact result (2) only by the constant leading factor of 4. The real transition temperature is lower than that predicted by this method because interactions between the loops act to reduce the energies at large perimeters.

Thus we interpret the transition to the paramagnet as deconfinement of localized composite excitations. The state becomes disordered when the loop size becomes comparable with the spacing between loops.

The magnetization and correlation lengths may also be calculated in similar series (see the Appendix). The magnetization M_0 may be used to calculate the fraction of spins opposed to the mean spin,

$$n_s = \frac{1-M_0}{2} = \frac{e^{-8D/T}}{256\sinh^4(2J/T)}. \tag{15}$$

Assuming that the lowest lying excitations are rectangular domains with four excited plaquettes per domain, we expect a relation of the form $n_s = (n_p/4)(n_b/n_p)^2$. We see that this is true for small J/T [recall that (J/T) is a small number, although expansions about $J=0$ are not valid in general since we are in an ordered phase].

Thus we have arrived at the following picture of the thermodynamics of the SEV model. There is a density of excited plaquettes n_p, which sit on the corners of overlapping closed loops. The total loop perimeter is measured in terms of the parameter n_b: the point $n_b=(1/2)$ is the maximally disordered spin field, in which the excited plaquettes are free. Away from the critical region (which is narrow), the excited plaquettes are nearly free in the paramagnetic phase: in the ferromagnetic phase they are confined on corners of rectangular loops whose typical size is much smaller than their inverse density.

So far, our microscopic arguments have been purely thermodynamic: we have not considered any dynamics. In the next section, we investigate the dynamics of the SEV model.

III. DYNAMICS

This section contains the key results of this paper. We briefly describe the dynamics of the paramagnetic state, which are essentially independent of J. We then discuss the onset of ordering as the temperature is lowered through T_c. We will find that supercooled states exist near T_c, which are well described by a simple "mobility field" picture for times shorter than their lifetime. We then discuss the extent to which these states can be regarded as metastable, and what determines their lifetimes.

We begin with a very brief review of the dynamics in the paramagnetic state with $T<T_o$. Since J may be treated perturbatively in this regime, we write the Hamiltonian as in Eq. (3). Flipping a single spin involves flipping of the four plaquette variables adjacent to that spin. Thus spins adjacent to four unexcited plaquettes have a flipping rate that is suppressed by a factor $e^{-8D/T}$. However, the flip rate of spins adjacent to exactly one excited plaquette are suppressed only by a factor $e^{-4D/T}$. The excited plaquettes mark mobile regions in which spin flips are rather likely. Thus the model resembles kinetically constrained systems such as the FA model [9].

The relaxation time of the spins depends on the temperature and on the density of excited plaquettes, according to $\tau \sim n_p^{-1}e^{4D/T}$. This arises from localized one-dimensional diffusion of pairs of excited plaquettes [20,21]. In equilibrium, we have $n_p \simeq c = e^{-2D/T}$, so the relaxation time diverges as c^{-3}. More precisely, we have the scaling relation [20]

$$\langle \sigma_{ij}(t_w)\sigma_{ij}(t+t_w)\rangle_{c,\mathrm{eq}} = f(c^3 t) \tag{16}$$

for the on-site autocorrelation function in equilibrium at a given value of c. This is strong glass behavior in the classification of Angell [22].

We now turn to results for the SEV model below T_c, where J may not be treated perturbatively. We discuss the phenomenological similarities and differences between this model and physical glass formers. We then interpret this behavior with the aid of mean field rate equations.

A. Existence of supercooled states

We start this section by demonstrating how a supercooled state may be formed below T_c. We investigate the dynamics of the system by means of simulations which use a continuous time Monte Carlo algorithm [23], with periodic boundary conditions. The number of excited plaquettes in each row and column is constrained to be even in this treatment, so the linear size of the system must be greater than $(2/n_p)$ for

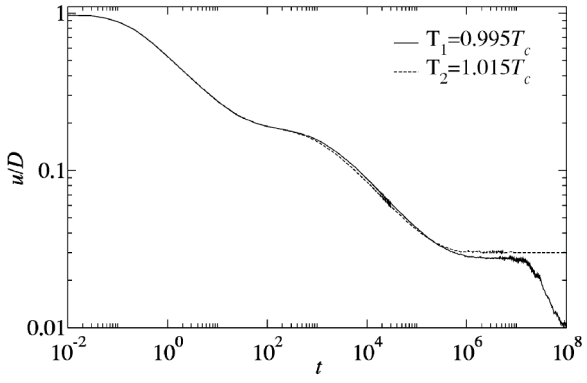

FIG. 3. Behavior of the system after two quenches from infinite temperature to just below and just above $T_c=0.45D$. The two plateaux correspond to the onset of activated dynamics, and equilibration in the disordered (glassy) state. However, the disordered state is unstable below T_c, as is clear at longer times.

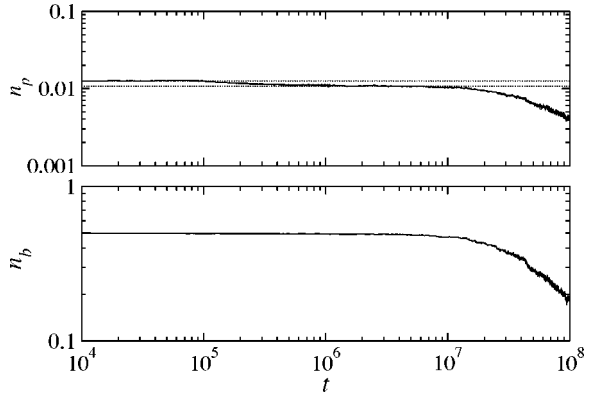

FIG. 4. Behavior of the SEV model after a quench from $T_1=1.02T_c$ to $T_2=0.996T_c$ with $T_c=0.45D$. We show concentrations of excited plaquettes, n_p, and broken bonds, n_b. The dotted lines mark $c_{1,2}=e^{-2D/T_{1,2}}$.

reliable results. Some of the main features of the dynamics of the SEV model are shown in Fig. 3. We measure the energy density of the system with respect to the ground state:

$$u = \langle H/N \rangle + D + 2J. \tag{17}$$

The dashed trace in Fig. 3 shows the internal energy density after quenching to a temperature T_1 such that $T_c<T_1<D$. After an initial transient, the system ages in a power law fashion toward equilibration at $u\sim 2De^{-2D/T_1}+2J$. The plateau at $(u/D)\simeq 0.2$ is a characteristic feature of models with kinetic constraints (whether explicit [9] or emergent [16,24]). It represents the onset of "activated" dynamics. The equilibration time for the paramagnet scales as a power of $c=e^{-2D/T}$. All these features are seen in the model with $J=0$ [15,17].

In contrast, the full trace in Fig. 3 shows the behavior on quenching to a temperature T_2 satisfying $T_2<T_c<D$, but with T_2 close to T_c. The behavior resembles that of the quench to T_1, including apparent equilibration at $u\sim 2De^{-2D/T_2}+2J$. However, this state is not stable, and the energy falls further at longer times. This behavior resembles that of glass formers, where the state on the lower plateau would be called a supercooled liquid. The behavior is also qualitatively similar to that observed in Ref. [12].

In order to focus on the supercooled states, we show further simulations in Fig. 4. The system is cooled through T_c in a single small step. We plot n_p and n_b as functions of time. From the plot of n_p, we see that the density of free excitations responds relatively quickly to the change in temperature: it falls from $c_1=e^{-2D/T_1}$ to $c_2=e^{-2D/T_2}$, where it appears to stabilize.

The response of n_b to the cooling is much slower. Recall that this correlation function measures the clustering of excited plaquettes. This clustering is a much slower process than the creation and annihilation steps leading to a change in the concentration of excitations. Looking at the late times in Fig. 4 when the clustering does start to occur, the system ages towards the ferromagnetic state with both n_p and n_b falling together. Taking the two traces in Fig. 4 together, we see that there are two separate time scales: one is associated with changes in n_p, the other with changes in n_b.

Turning to the supercooled state itself, it is clear from Fig. 4 that it has $n_p\simeq c=e^{-2D/T}$ and $n_b\simeq(1/2)$. This resembles closely the state that would be formed if we set $J=0$ in the Hamiltonian. Thus the effect of the interactions between plaquettes (the term proportional to J in the Hamiltonian) is to set the lifetime of the supercooled state. The properties of the state itself are independent of J. We conclude that the supercooled state in the SEV model can be well described by the much simpler plaquette model of Eq. (3): a kinetically frustrated model with trivial thermodynamic properties. This is the assumption made when describing glass formers by simple models of dynamical heterogeneity [1,3]: in the SEV model, this assumption seems to be reasonable.

A key property of supercooled states is that two-time correlation functions should be stationary within the supercooled state. That is, expectation values of the form $\langle A(t_w)A(t+t_w)\rangle$ should be independent of t_w as long as $(t+t_w)$ is less than the lifetime of the states. In Fig. (5), we show that the supercooled state with $n_p=c$ and $n_b=(1/2)$ has this property. Since the excited plaquettes are uncorrelated in this state, it may be prepared manually, without the need for simulation. Further, the single-spin autocorrelation function in the supercooled state is the same as that in the model with $J=0$ at the same temperature. It therefore obeys the dynamical scaling law of Eq. (16), and is independent of J.

As a final comment on Fig. 5, we note that the criterion that the supercooled state should be long lived is satisfied, since stationarity holds over time scales much longer than the single-spin relaxation time. Thus the data in that figure are consistent with the picture of a supercooled state that appears to equilibrate in a metastable basin.

B. Lifetime of supercooled states

Having identified a supercooled state at temperatures near T_c, we now proceed to discuss its lifetime. We prepared states with $n_p=c$ and $n_b=(1/2)$ and measured the time taken for n_b to fall to 0.45. Results are shown in Fig. 6. The lifetime gets very large both near T_c, and in the limit $T\to 0$.

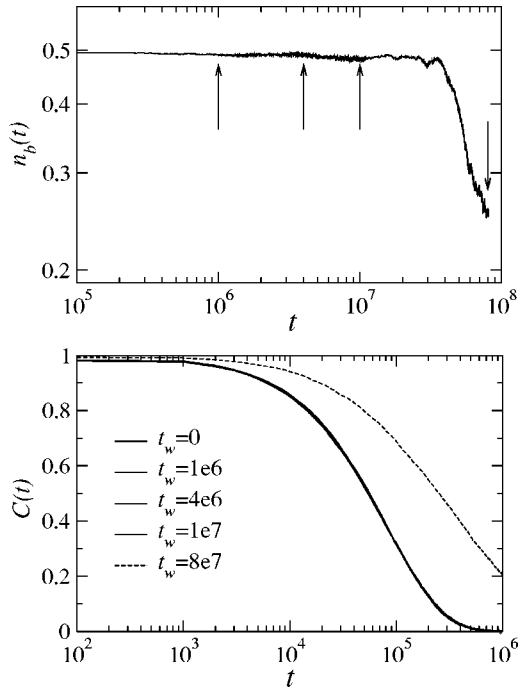

FIG. 5. (Top) Fraction of broken bonds against waiting time in the supercooled state: $T=0.996T_c$, $T_c=0.444D$. (Bottom) Autocorrelation function $C(t)=\langle\sigma_{ij}(t+t_w)\sigma_{ij}(t_w)\rangle$ for the waiting times marked in the top figure. The two-time function appears stationary until the system starts to nucleate at around 3×10^7 Monte Carlo sweeps.

Near T_c, the states are supercooled. At very low temperatures, the lifetimes are similarly long, but in this case they are of the same order as the spin relaxation time. These states are not equilibrated in a metastable basin; rather, their long lifetimes reflect the drastic slowing down of all time scales as the temperature is reduced.

From Fig. 6, we conjecture that the nucleation time has the form

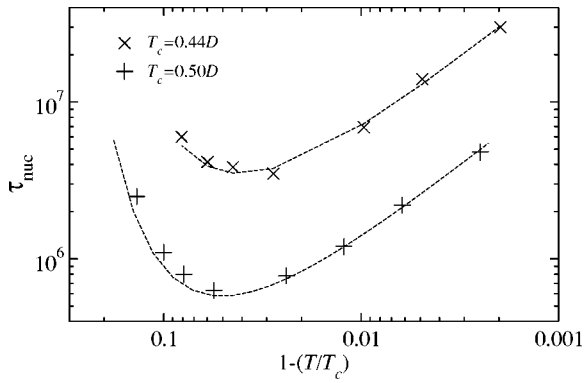

FIG. 6. Nucleation times at $T_c=0.50D$ and $T_c=0.44D$, measured by averaging over several runs similar to those in Fig. 5. The temperature increases from left to right, but note that the zero of the logarithmic scale is at T_c, away to the right. The dashed lines are fits to the form of Eq. (18) using the same value of $\gamma=0.17$. This form captures the qualitative features of the curve: a power law increase near T_c and an exponential divergence at low temperatures.

$$\tau_{\rm nuc}=\gamma e^{2D/T_c}\frac{e^{4D/T}}{1-(T/T_c)} \tag{18}$$

where γ is a (microscopic) rate that depends only weakly on T and T_c. Physically, the nucleation rate is suppressed by a Boltzmann factor that arises from the activated dynamics, and by a factor of $\Delta\mu/T\simeq(T_c/T)-1$, where $\Delta\mu$ is the free energy difference between ordered and disordered phases.

In other words, behavior near T_c is characterized by a separation of the nucleation time from the relaxation time τ. The minimum in the nucleation time occurs at

$$T_x=T_c[1-(T_c/4D)+O(T_c/D)^2]. \tag{19}$$

The relaxation time in the paramagnet is given approximately by $\tau=0.14e^{6D/T}$, so at the minimum we have $\tau^*\simeq0.14e^{(6D/T_c)+(3/2)}$ and $\tau^*_{\rm nuc}\simeq0.17(4D/T_c)e^{(6D/T_c)+1}$. The result is that $\tau^*_{\rm nuc}>\tau^*$ as long as $T_c<T_o\sim D$, which is the regime of interest in this section. The two time scales are well separated for all temperatures between T_x and T_c.

This separation results from the small amount of free energy that is released on ordering. States in which these times are well separated are "supercooled" in the sense that the degrees of freedom associated with the relaxation time appear to equilibrate in a state that is known to be unstable at long times.

At very low temperatures, we see that $\tau_{\rm nuc}$ will become smaller than the extrapolated relaxation time $\tau_{J=0}\sim e^{6D/T}$. The result is that the physical relaxation time at low temperatures is smaller than $e^{6D/T}$. The dynamics of the aging state are faster than those of a similar state with $J=0$.

These results may be interpreted in the picture of the model as a combination of a zero-temperature dynamical fixed point and a finite temperature thermodynamic singularity. The spin relaxation time is controlled by the activated dynamics associated with the zero-temperature fixed point. It is large compared to microscopic time scales, but small compared to the lifetime of the supercooled state. That lifetime is very long near the thermodynamic transition: the slowing down is due to the small free energy difference between paramagnetic and ferromagnetic states. We comment here that "soft modes" at large length scales are not relevant to the behavior observed in simulations, due to the narrowness of the critical region.

While supercooled states are familiar in systems with first order phase transitions, they are not usually observed near second order transitions, such as the one discussed in this work. In first order systems, the nucleation time may be predicted by thermodynamic arguments. The free energy of a (d-dimensional) droplet of ordered phase in a disordered background is approximately $\sigma r^{d-1}-\Delta\mu r^d$ where r is the linear size of the droplet, σ the surface tension, and $\Delta\mu$ the free energy difference between the two phases. Thus, nucleation requires the formation of a droplet of linear size $r^*\sim\sigma/\Delta\mu$, with an associated free energy barrier proportional to $\Delta\mu^{-1}$ (in two dimensions). The nucleation rate is therefore suppressed by a factor $e^{-\sigma^2/T\Delta\mu}$. This is exponential suppression of nucleation.

From Eq. (18), we see that the SEV model has linear suppression: the nucleation rate is proportional to $\Delta\mu$. This

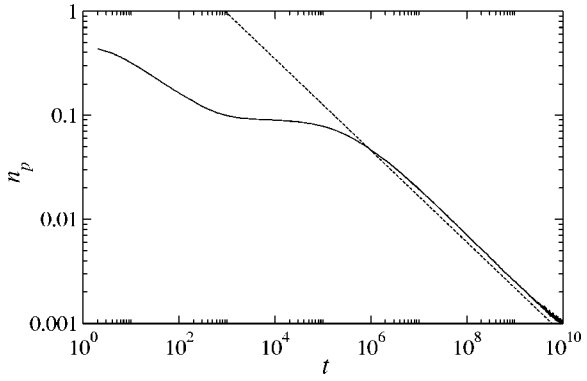

FIG. 7. Plot showing aging of the paramagnet. We plot n_p as a function of time after a quench from infinite temperature to $T=0.286D$, with $J=0$. The dashed line is a guide to the eye, corresponding to a decay proportional to $t^{-0.45}$.

second order system has weaker suppression than that predicted for first order systems. Since the transition in the SEV model is second order, there are processes by which the bulk of the system may be continuously changed from paramagnet to ferromagnet, without a large free energy barrier. These processes are slow because they require cooperative motion of many spins, but the exponential slowdown that would result from a high energy intermediate state is not observed. While the phenomenology of the SEV model resembles that of first-order systems, the lifetimes of supercooled states tend to be shorter than those in systems with diverging free energy barriers near T_c. In this respect, the SEV model is an imperfect model of a glass former. However, we argue that the free energy barrier between ordered and disordered states in first order systems should mean that the supercooled states are less affected by the critical point than those of the SEV model. Thus, if the thermodynamic singularity is largely irrelevant in this model, then we expect it to be even less relevant in similar first order systems.

C. Rate equation approach and aging behavior

In order to understand the results of the previous section, we give a brief discussion of the aging behavior of the system. We parametrize this behavior in terms of mean field rate equations for the observables n_p and n_b. This will provide further evidence that the supercooled states are characterized by fast dynamics for the concentration of excited plaquettes, n_p, combined with much slower dynamics for their spatial ordering (measured by n_b).

In paramagnetic states with $T<D$, the equilibrium value of n_b is 0.5 and that of n_p is $c \simeq e^{-2D/T}$. Aging toward equilibrium occurs at $n_b=0.5$, with $n_p \sim t^{-0.45}$ (a sample trace is shown in Fig. 7, but the observed exponent is independent of temperature, as long as we work between T_c and T_o). The rate is limited by the slow diffusion of excited plaquettes (there is no simple diffusive process for isolated excitations).

There are two regimes for the aging toward the ferromagnetic state. We define T_x as the temperature at which the nucleation time is minimal (recall Fig. 6). As shown in Fig. 3, after quenching to T near T_c ($T>T_x$), the system appears

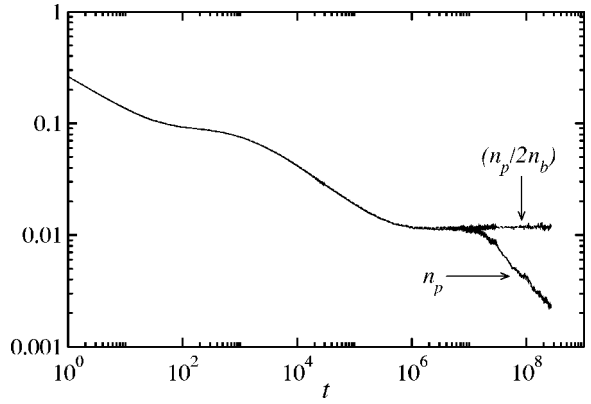

FIG. 8. Aging of the system at a temperature $T=0.995T_c$. We have $T_c=0.451D$ so that $T>T_x$. We plot n_p and $n_p/2n_b$ after a quench from infinite temperature. Both quantities are equal until the supercooled state becomes unstable. At these long times, n_p decreases, but the ratio $n_p/2n_b$ remains constant with a value approximately equal to $c=e^{-2D/T}$.

to equilibrate at $n_p=c$ (with $n_b=0.5$), before aging toward the ferromagnetic state. In Fig. 8 we show a similar scenario, but continuing to slightly longer times. At these long times, the system ages with the ratio $(n_p/2n_b) \simeq c$. The decrease of n_b happens on the long time scale given by $\tau_{\rm nuc}$. However, the plaquette concentration n_p is reacting on a much faster time scale. The interpretation is that n_p has stabilized in an environment set by the current value of n_b. It seems that the stable value of n_p is around $2cn_b$.

If instead we quench to a temperature below T_x, there is no apparent equilibration at $n_p \simeq c$. Instead, the effect of finite J becomes apparent when $n_p \simeq e^{-2D/T_c} > c$. There is a transient effect as n_b begins to change, but the long time behavior again has a constant ratio $(n_p/2n_b) \simeq 0.8e^{-2D/T_c}$ (see Fig. 9). Simulations indicate that the constant value of $(n_p/2n_b)$ seems to depend on T_c as shown, and to vary only weakly with T. Further, the exponent associated with the aging appears to be similar to that in the paramagnetic state (around 0.45). The natural interpretation is that the aging of these states is controlled in the same way as the aging of the paramagnet: by the slow diffusion of excited plaquettes. The

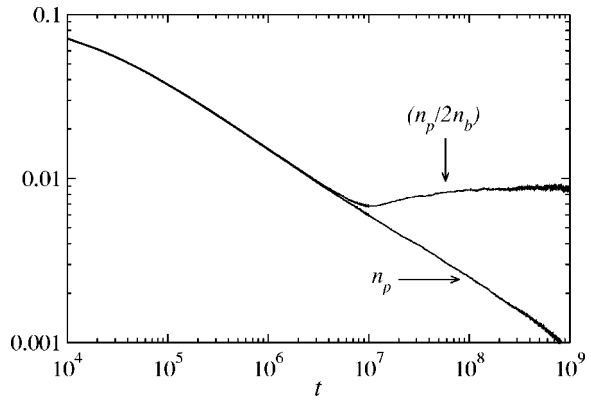

FIG. 9. Aging at $T=0.364D$, with $T_c=0.444D$, so that $T<T_x$. The ratio $n_p/2n_b$ deviates from n_p at a value around e^{-2D/T_c}, so the system does not reach the supercooled state with $n_p=c=e^{-2D/T}$.

dynamics of n_b are now faster than those of n_p, and the spatial ordering of the excited plaquettes is responding faster than the plaquette density.

This description of the aging behavior is consistent with the following conjectured rate equations:

$$e^{4D/T}\partial_t n_p = \lambda_p n_p^{2.2}(2cn_b - n_p), \tag{20}$$

$$e^{4D/T}e^{2D/T_c}\partial_t n_b = \lambda_b n_b[1-(T/T_c)](X_b - 2n_b), \tag{21}$$

where $X_b = \min(1, n_p A e^{2D/T_c})$. The significance of this quantity is that n_b would equilibrate to $X_b/2$ if the concentration of plaquettes were constrained to be equal to n_p. The exponent 2.2 in Eq. (20) is fixed by the exponent 0.45 for the power law decay of the energy in the paramagnetic phase (as shown in Fig. 7). The overall scaling of time with temperature in that equation is also fixed by the aging of the paramagnetic states. The scaling of time in Eq. (21) is determined by the scaling of the nucleation time in Eq. (18).

The adjustable parameters of the theory are therefore the rates λ_p and λ_b, and the constant A. The two rates are microscopic frequencies reflecting the cooperative motion of the spins required to change n_p or n_b. The constant A determines the ratio of n_b and n_p when the aging is controlled by plaquette diffusion (as in Fig. 9). The instability of the supercooled state means that $Ae^{2D/T_c} < e^{2D/T}$: the data of Fig. 9 are consistent with $(1/A) \simeq 0.8$, as mentioned above.

We make no attempt to justify these rate equations on microscopic grounds. For example, the exponent 2.2 in Eq. (20) is a nontrivial decay exponent for an annihilation-diffusion problem in which diffusion of single excited plaquettes is suppressed by the kinetic constraint. We imagine "integrating out" all the microscopic degrees of freedom: the effect of the complicated fluctuation effects appears only in this exponent. However, while their microscopic origin is unclear, the interesting features of these equations are (1) the different temperature scaling of the times associated with the two degrees of freedom, and (2) the presence of points at which one degree of freedom is not changing. The first feature leads to a separation of time scales in the problem. When this is combined with the second feature, the apparent metastability of the supercooled states becomes possible. In this case, the faster degree of freedom is n_p, which equilibrates at $2cn_b$ on a time scale that is fast enough that n_b can be considered to be constant. The aging of the supercooled state then has a time scale determined by the rate equation for n_b. That degree of freedom is trying to reach apparent equilibration at $n_p A e^{2D/T_c}/2$, but n_p is the faster degree of freedom, and is moving the target downward just as fast as n_b decreases toward it. This results in the aging at constant n_b/n_p that is shown in Fig. 8. An exactly analogous process is taking place in Fig. 9, except that n_p is now the slow degree of freedom.

The central point of the above argument is that the slow degrees of freedom set a "target value" for the fast ones, at which the fast degrees of freedom appear to equilibrate when viewed on the fast time scale. This is the sense in which the states discussed in the previous section are "supercooled." Their lifetime is then set by the slow degrees of freedom, and this lifetime is much longer than relaxation time scales in these states. To understand the correlations in the aging state, it would be desirable to study the thermodynamics of the excited plaquettes while working at fixed n_b. However, this is well beyond the scope of this paper.

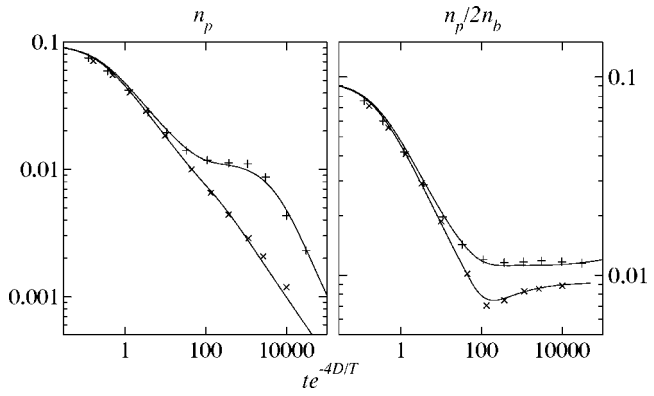

FIG. 10. Fit to the data of Figs. 8 (+ symbols) and 9 (× symbols) using mean field rate equations (20) and (21). Note that the left and right panels each show data from two runs, showing how the different regimes are captured by the same rate equations. Parameters are $(\lambda_p, \lambda_b, A) = (350, 17, 0.85)$ for the data of Fig. 8, and $(\lambda_p, \lambda_b, A) = (350, 17, 1.20)$ for those of Fig. 9.

Note that there is no provision in Eqs. (20) and (21) for equilibration in a ferromagnetic state. However, the large internal energy difference between paramagnetic and ferromagnetic states means that this equilibration is not observed on time scales that are accessible in simulation. Therefore, Eqs. (20) and (21) appear to be valid over time scales that are several orders of magnitude longer than the lifetimes of the supercooled states.

It is simple to verify that the qualitative behavior of Figs. 4 and 7–9 may be fitted by Eqs. (20) and (21), with appropriate values of $(\lambda_p, \lambda_b, A)$. See Fig. 10, in which we show reasonable agreement. Note, however, that the onset of nucleation from the supercooled state is more sudden than that predicted by the mean field equations. The initial ordering is slower than the power law predicted by these simple rate equations.

The requirement of different parameters to fit the different simulations in Fig. 10 show the rather simplistic assumptions for the temperature scaling in the mean field equations. That is, the linear suppression of the nucleation rate with $(T_c - T)$ is valid only near T_c, necessitating adjustment of λ_b at smaller temperatures. We have already commented that A will be temperature dependent, but that this dependence has a weaker effect on X_b than the exponential dependence of that quantity on T_c.

The fits of Fig. 10 using these mean field equations support our interpretation of Fig. 6 in terms of purely dynamical effects that do not depend on thermodynamic quantities like free energy barriers and spinodal points.

IV. DISCUSSION AND CONCLUSIONS

We have shown that the SEV model can be interpreted in terms of a high temperature state in which excitations are

free and pointlike, and a low temperature phase in which these free excitations are confined into composite objects, with a characteristic size that is smaller than their spacing. The dynamics of the paramagnet are well described in a mobility field picture similar to the FA model.

Near the transition to the ordered phase, supercooled paramagnetic states have long lifetimes. Two-time correlation functions show stationarity in these states, and both their dynamics and their thermodynamics are well described by the plaquette model. However, these states have finite lifetimes, beyond which stationarity is lost and it becomes clear that they are unstable to the ferromagnetic state. This situation resembles the situation in physical glass formers, except that the presence of a first order transition in those systems means that the lifetimes of the supercooled states diverge much faster near T_c than in the SEV model.

We have also shown that the mean field rate equations (20) and (21) are a suitable framework for describing the out of equilibrium (aging) behavior of the SEV model.

We end this work with some comments about the significance of these results in the context of the literature. Comparing with the work of Cavagna *et al.* [12], we note the similarity between the phenomenology of their model and the SEV model. However, the exact solution of the eight-vertex model, and the understanding of the dynamics of the paramagnetic state that arises from previous work on the plaquette model allow us to investigate the behavior from a more microscopic viewpoint.

We illustrate this with three points. First, the internal energy of the SEV model changes very rapidly around T_c. From simulation evidence alone, we might (erroneously) conclude that the transition was first order. However, we know from theoretical considerations that the transition is second order. This knowledge is important when discussing the possible metastability of supercooled states. Second, the power law suppression of nucleation near T_c in the SEV model results from the fact that our transition is second order. For a first order transition we would expect an exponential suppression. The nature of this suppression in Ref. [12] does not seem to be clear. And finally, we are able to identify the minimum in Fig. 6 as arising not from the crossing of a spinodal, but rather from a crossover in time scales.

We would also like to point out some similarities between the paramagnetic phase of the SEV model and the models which are conjectured to be controlled by the behavior of entropic droplets [7,25]. As mentioned above, the invariance of the Hamiltonian at $J=0$ under flipping a whole row or column of spins leads to a large (but nonextensive) ground state entropy. We have shown that the introduction of J is largely irrelevant above T_c and in the supercooled states. Therefore, we may interpret the low temperature paramagnetic states ($T_c < T \ll T_o$) as a mosaic of the many $J=0$ ground states. The "droplets" are referred to as "entropic" in this scenario. This name arises because there does not seem to be an energetic argument for their stability, so it is assumed that they are stabilized by some entropic mechanism. In the plaquette model, the borders between droplets of each ground state are not one dimensional as one might expect, but rather arise from pointlike excited plaquettes. This situation was alluded to in the recent paper of Bouchaud and Biroli [25]. Since there is no perimeter for a surface tension to couple to, the entropic forces are strong enough to stabilize the mosaic state. This is the situation in the SEV model at finite J, but $T > T_c$.

If we accept the plaquette model as a realization of the entropic droplet picture, it is interesting to note that the only fixed point in that model is at zero temperature. That is, although the entropy falls rapidly as the temperature is reduced through T_o, any extrapolation that leads to $S=0$ at a finite temperature is not valid. Rather, the entropy remains regular at all temperatures (even those in which the glassy phase is completely unstable to the crystal). In fact, $S_{\text{glass}} > S_{\text{crystal}}$ all the way down to $T=0$ (where S_{glass} is the entropy associated with the plaquette model and S_{crystal} is the entropy of the SEV model with the same value of D and at the same temperature). In this scenario the Kauzmann paradox [22] is seen as arising from an unphysical linear extrapolation of the glassy entropy.

To conclude, we have shown that the plaquette model limit of the SEV model describes its behavior in both stable and supercooled paramagnetic states. This model resembles both the mobility field description of glassy systems (as exemplified by the FA model) and the entropic droplet picture. However, there is no finite temperature fixed point in the theory of the glassy states; thus Kauzmann's paradox is avoided. Taken together, these results are further evidence that theories without thermodynamic singularities at finite temperature are suitable for describing glassy states [1–3].

ACKNOWLEDGMENTS

We thank A. Cavagna, D. Chandler, and S. Whitelam for discussions. We acknowledge financial support from EPSRC Grants No. GR/R83712/01 and No. GR/S54074/01 and University of Nottingham Grant No. FEF 3024.

APPENDIX: LOW AND HIGH TEMPERATURE EXPANSIONS OF THE EIGHT-VERTEX MODEL

In this appendix, we consider the series for the free energy given by Baxter [19]:

$$(f/T) = -\ln c' - \sum_m \frac{x^m[(q/x^2)^m - 1]^2(1-x^m)^2}{m(1-q^{2m})(1+x^{m/2})} \qquad \text{(A1)}$$

where q, x^2, and c' depend on the model parameters D/T and J/T. The parameter z in Baxter's calculation is 1 in the SEV model since the Hamiltonian is invariant under 90° rotations. The dependence of q and x^2 on the original parameters (D,J) is rather indirect: the main task of this appendix will be to derive simple relations between (q,x^2) and $(D/T,J/T)$ in the ferromagnetic phase.

However, we first consider the contribution of the $\ln c'$ term to the free energy. In the paramagnetic phase we have

$$(f_{\text{PM}}/T) \sim \ln c' = \ln[e^{D/T}\cosh^{2J/T} + e^{-D/T}] \qquad \text{(A2)}$$

which is the result quoted as Eq. (5), and may be used to calculate properties of the paramagnetic phase. However, in the ferromagnetic phase we have $c' = e^{(D+2J)/T}$, so taking only

the leading term leads to the trivial result $n_p = n_b = 0$. There are no excitations in the ferromagnetic phase at this order. We must therefore estimate the parameters x and q in this phase.

The prescription for calculating these parameters is given by Baxter [19], but we give a brief review. The ratios D/T and J/T are used to calculate four parameters (a,b,c,d). The partition function is symmetric under interchange of the four quantities $(a \pm b, c \pm d)$. We may therefore map the parameters into the principal regime, to give (a',b',c',d') satisfying $c'+d' > c'-d' \geqslant a'+b' > a'-b' \geqslant 0$. These parameters are used to calculate $\Delta = [-(c'^2+d'^2)+(a'^2+b'^2)]/(2c'd' + 2a'b')$ and $\gamma = (c'd'/a'b')$.

In the ferromagnetic phase we have $\gamma = \exp(4D/T)$. We work at $T_c < D$ so γ is a very large number, and we arrive at

$$\Delta = \cosh(4J/T)\left[1 - \gamma^{-1}\left(1 + \frac{1}{\cosh(4J/T)}\right) + O(\gamma^{-2})\right]. \tag{A3}$$

The next step is to calculate the parameter k, from

$$\gamma(1+k^2) = \Delta^2(1+\gamma)^2 - (1+\gamma^2) \tag{A4}$$

and the result is

$$k = \frac{e^{-4D/T}}{2\sinh^2(2J/T)[1+\cosh(2J/T)]} + O(\gamma^{-2}). \tag{A5}$$

We have $0 < k < 1$, and k is the elliptic modulus with nome q. That is,

$$-\ln q \int_0^1 \frac{dt}{\sqrt{1-t^2}\sqrt{1-k^2t^2}} = \pi \int_0^\infty \frac{dt}{\sqrt{1+t^2}\sqrt{k^2+t^2}}. \tag{A6}$$

For the series of (A1) to converge quickly, we require $q < 1$: in that case Eq. (A6) reduces to $q \simeq (k^2/16)$, and therefore we have the approximate relation

$$q \simeq \frac{e^{-8D/T}}{128\sinh^4(2J/T)}, \tag{A7}$$

whose condition for validity is that k be small, which requires that $\sinh(2J/T) \ll e^{-2D/T}$. This is the condition that we are well inside the ferromagnetic phase, as is clear from Eq. (2).

In order to evaluate the terms in (A1), we also require an approximate form for x. The definition of x is

$$\ln\left(\frac{q}{x^2}\right)\int_0^1 \frac{dt}{\sqrt{1-t^2}\sqrt{1-k^2t^2}} = \int_{\sqrt{\gamma k}}^\infty \frac{\pi\, dt}{\sqrt{1+t^2}\sqrt{k^2+t^2}}, \tag{A8}$$

from which the relation $x^2 < q$ is clear. This integral may be expanded in a series around $(1/\sqrt{\gamma k}) = 0$. Equation (A5) shows that this parameter is small if $J \ll T$. The result is that

$$(q/x^2) - 1 \simeq 4\sinh(2J/T). \tag{A9}$$

Substituting into (A1), and ignoring all terms with $m \geqslant 2$, we arrive at

$$f_{\mathrm{FM}} \simeq -(D/T) - (J/T) - \frac{e^{-8D/T}}{16\sinh^2(2J/T)} \tag{A10}$$

which gives the result (11), qualified by the validity condition

$$e^{-2D/T} \ll \sinh(2J/T) \ll 1, \tag{A11}$$

from which we note that this is not an expansion about $T = 0$, but rather a useful approximation to the free energy in this part of the parameter space.

[1] J. P. Garrahan and D. Chandler, Phys. Rev. Lett. **89**, 035704 (2002); Proc. Natl. Acad. Sci. U.S.A. **100**, 9710 (2003).
[2] S. Whitelam, L. Berthier, and J. P. Garrahan, Phys. Rev. Lett. **92**, 185705 (2004).
[3] L. Berthier and J. P. Garrahan, J. Chem. Phys. **119**, 4367 (2003); Phys. Rev. E **68**, 041201 (2003).
[4] W. Götze and L. Sjögren, Rep. Prog. Phys. **55**, 55 (1992).
[5] G. Biroli and J. P. Bouchaud, Europhys. Lett. **67**, 21 (2004).
[6] D. Kivelson, S. A. Kivelson, X. L. Zhao, Z. Nussinov, and G. Tarjus, Physica A **219**, 27 (1995).
[7] X. Xia and P. G. Wolynes, Proc. Natl. Acad. Sci. U.S.A. **97**, 2990 (2000).
[8] M. Mézard and G. Parisi, Phys. Rev. Lett. **82**, 747 (1999); S. Franz and G. Parisi, J. Phys. C **12**, 6335 (2000).
[9] G. H. Fredrickson and H. C. Andersen, Phys. Rev. Lett. **53**, 1244 (1984).
[10] J. Jäckle and S. Eisinger, Z. Phys. B: Condens. Matter **84**, 115 (1991).
[11] F. Ritort and P. Sollich, Adv. Phys. **52**, 219 (2003).
[12] A. Cavagna, I. Giardina, and T. S. Grigera, Europhys. Lett. **61**, 74 (2003); J. Chem. Phys. **118**, 6974 (2003).
[13] S. Franz, M. Mezard, F. Ricci-Tersenghi, M. Weigt, and R. Zecchina, Europhys. Lett. **55**, 465 (2001).
[14] M. R. Swift, H. Bokil, R. D. M. Travasso, and A. J. Bray, Phys. Rev. B **62**, 11 494 (2000).
[15] A. Lipowski, J. Phys. A **30**, 7365 (1997).
[16] J. P. Garrahan and M. E. J. Newman, Phys. Rev. E **62**, 7670 (2000).
[17] J. P. Garrahan, J. Phys.: Condens. Matter **14**, 1571 (2002).
[18] Y. Brumer and D. R. Reichman, Phys. Rev. E **69**, 041202 (2004).
[19] R. J. Baxter, *Exactly Solved Models in Statistical Mechanics* (Academic Press, London, 1982).
[20] A. Buhot and J. P. Garrahan, Phys. Rev. Lett. **88**, 225702

(2002).
[21] D. Espriu and A. Prats, Phys. Rev. E **70**, 046117 (2004).
[22] C. A. Angell, Science **267**, 1924 (1995).
[23] M. E. J. Newman and G. T. Barkema, *Monte Carlo Methods in Statistical Physics* (Oxford University Press, Oxford, 1999).
[24] L. Davison, D. Sherrington, J. P. Garrahan, and A. Buhot, J. Phys. A **34**, 5147 (2001).
[25] J.-P. Bouchaud and G. Biroli, J. Chem. Phys. **121**, 7347 (2004).